Complex Correspondence Principle

Carl M. Bender,[1] Daniel W. Hook,[2] Peter N. Meisinger,[1] and Qing-hai Wang[3]
[1]*Department of Physics, Washington University, St. Louis, Missouri 63130, USA*
[2]*Theoretical Physics, Imperial College London, London SW7 2AZ, United Kingdom*
[3]*Department of Physics, National University of Singapore, Singapore 117542*
(Received 10 December 2009; published 12 February 2010)

Quantum mechanics and classical mechanics are distinctly different theories, but the correspondence principle states that quantum particles behave classically in the limit of high quantum number. In recent years much research has been done on extending both quantum and classical mechanics into the complex domain. These complex extensions continue to exhibit a correspondence, and this correspondence becomes more pronounced in the complex domain. The association between complex quantum mechanics and complex classical mechanics is subtle and demonstrating this relationship requires the use of asymptotics beyond all orders.

DOI: 10.1103/PhysRevLett.104.061601 PACS numbers: 11.30.Er, 02.30.Fn, 03.65.−w, 05.40.Fb

The correspondence principle states that at high energy quantum mechanics resembles classical mechanics. Figure 1 illustrates this resemblance for the harmonic-oscillator Hamiltonian $H = p^2 + x^2$ by comparing the quantum probability density $\rho_{\text{quantum}}(x) = |\psi_{16}(x)|^2$ for the 16th energy level $E_{16} = 33$ with the classical probability density $\rho_{\text{classical}}(x) = 1/s$, where s is the speed of the particle. In the classically allowed region, which is bounded by the turning points at $\pm\sqrt{33}$, $\rho_{\text{quantum}}(x)$ oscillates about $\rho_{\text{classical}}(x)$. At the turning points $\rho_{\text{classical}}$ is singular because s vanishes, but $\rho_{\text{classical}}$ is normalizable because this singularity is integrable. In the classically forbidden region ρ_{quantum} decays exponentially; in conventional classical mechanics the particle cannot enter this region and thus $\rho_{\text{classical}}$ is thought to vanish.

This Letter generalizes quantum and classical probability into the complex domain. In complex classical mechanics we solve Hamilton's equations $\dot{x} = \frac{\partial H}{\partial p}$, $\dot{p} = -\frac{\partial H}{\partial x}$ for complex initial conditions and not just for initial conditions in the classically allowed region [1–7]. For the harmonic oscillator the classical orbits are nested ellipses with foci at the turning points. Using ρ_{quantum} in Fig. 1 as a guide, we require the probability of a classical particle being on more distant ellipses to decay exponentially, and we plot in Fig. 2 the relative probability density of finding the classical particle at the point $z = x + iy$.

Figure 2 shows that, contrary to the traditional view, the classical particle density in the classically forbidden region is actually nonzero, and that $\rho_{\text{classical}}$ resembles ρ_{quantum} in this region [8]. This figure emphasizes that the classical probability density extends beyond the real axis and into the complex plane, where $\rho_{\text{classical}}(x, y)$ falls off as the reciprocal of the distance from the origin.

To establish the complex correspondence principle we must continue the quantum probability density into the complex plane to match the complex classical probability density in Fig. 2; to do this we must extend quantum mechanics into the complex domain [9]. A Hermitian Hamiltonian ($H = H^\dagger$) has real energy levels and unitary time evolution. However, the class of physically allowable Hamiltonians may be extended to include non-Hermitian Hamiltonians that possess an unbroken $\mathcal{PT}$ (combined parity and time-reversal) symmetry [10–15]. These complex Hamiltonians also have real spectra and generate unitary time evolution, and such Hamiltonians have recently been observed in the laboratory [16–18].

The potential for $\mathcal{PT}$-symmetric Hamiltonians satisfies $V^*(-z) = V(z)$. This allows us to use the time-dependent Schrödinger equation $i\psi_t(z, t) = -\psi_{zz}(z, t) + V(z)\psi(z, t)$ to derive a local conservation law in the complex plane. The continuity equation is $\rho_t(z, t) + j_z(z, t) = 0$, where the local density and current are

$$\rho(z, t) \equiv \psi^*(-z, t)\psi(z, t) = [\psi(z, t)]^2, \tag{1}$$

$$j(z, t) \equiv i\psi_z^*(-z, t)\psi(z, t) - i\psi^*(-z, t)\psi_z(z, t). \tag{2}$$

This Letter considers only wave functions $\psi(z, t)$ that are eigenstates of H; for such states $\rho(z)$ is time independent

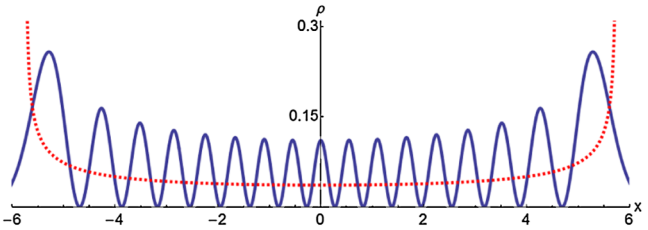

FIG. 1 (color online). Correspondence principle for the harmonic oscillator. The probability density $\rho(x) = |\psi_{16}(x)|^2$ for a quantum particle (solid curve) and the corresponding probability density for a classical particle of the same energy (dotted curve) are shown. In the parabolic potential well $\rho_{\text{quantum}}(x)$ is wavelike and oscillates closely about $\rho_{\text{classical}}(x)$. At the classical turning points, $\rho_{\text{classical}}(x)$ diverges. In the classically forbidden region the quantum particle density decays exponentially while the classical density is ordinarily assumed to vanish.

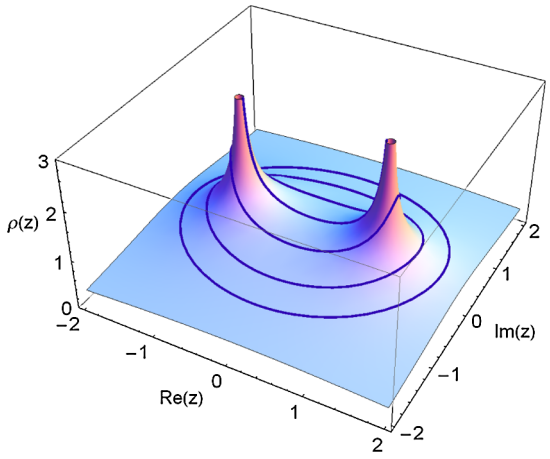

FIG. 2 (color online). Classical probability density at $z = x + iy$ in the complex plane for a particle of $E = 2$ in a harmonic potential. The probability density resembles a pup tent with infinitely high tent poles at the turning points. Classical trajectories are nested ellipses, all having the same period $T = \pi$. These complex orbits are superposed on the tent canopy. The degenerate ellipse, whose foci are the turning points at $\pm\sqrt{E}$, is the conventional real solution. Classical particles repeatedly cross the real axis in the classically forbidden regions $|x| > \sqrt{E}$.

and $j \equiv 0$. Note that $\rho(z)$ is analytic in the complex-z plane because it is not the absolute square of $\psi(z, t)$.

For a locally conserved probability density to be measurable it must be real and positive and its spatial integral must be normalized to unity; $\rho(z)$ satisfies a continuity equation, but $\rho(z)$ by itself cannot be a probability density because it is complex valued. Hence, we propose the novel approach of constructing a complex contour C on which $\rho(z)dz$ is an infinitesimal probability measure. Thus, we require that C satisfy the three conditions

$$\text{condition I:} \quad \mathrm{Im}[\rho(z)dz] = 0, \tag{3}$$

$$\text{condition II:} \quad \mathrm{Re}[\rho(z)dz] > 0, \tag{4}$$

$$\text{condition III:} \quad \int_C \rho(z)dz = 1. \tag{5}$$

For brevity, we discuss the harmonic-oscillator ground state $\psi_0(z) = e^{-z^2/2}$ for which $\rho(z) = e^{-x^2+y^2-2ixy}$. Since $dz = dx + idy$, condition I gives

$$dy/dx = \sin(2xy)/\cos(2xy), \tag{6}$$

which is a differential equation for the contour C. On the contour defined by this differential equation the local contribution $\rho(z)dz$ to the probability is real.

Next, we turn to condition III. Inserting (6) into (5), we get two forms for the probability integral:

$$I = \int_C dx \frac{e^{[y(x)]^2 - x^2}}{\cos[2y(x)x]} = \int_C dy \frac{e^{y^2 - [x(y)]^2}}{\sin[2yx(y)]}. \tag{7}$$

These integrals converge if the contour C terminates in the two good Stokes' wedges of opening angle $\pi/2$ centered about the real axis, but they diverge if C terminates in the bad Stokes' wedges of opening angle $\pi/2$ centered about the imaginary axis.

To determine whether the contour C terminates in good Stokes' wedges we must solve (6). However, this simple-looking differential equation does not possess a closed-form solution, and we must rely on asymptotic techniques. For large x the contour C approaches the center of the good Stokes' wedge and for large y, C approaches the center of the bad Stokes' wedge:

$$y(x) \sim n\pi/(2x) \qquad (x \to +\infty, n \in \mathbb{Z}), \tag{8}$$

$$x(y) \sim (m + 1/2)\pi/(2y) \qquad (y \to +\infty, m \in \mathbb{Z}). \tag{9}$$

This asymptotic analysis shows that the integration paths occur in quantized bunches labeled by the integers m or n. Higher-order asymptotic analysis reveals that these bunches are stable in the bad Stokes' wedges and unstable in the good Stokes' wedges. This means that as $|y| \to \infty$, a path in the bad Stokes' wedge is drawn towards the quantized curves in (9), but that as $|x| \to \infty$ paths veer away from the quantized curves in (8), which we call separatrices. Thus, only the isolated separatrices ever reach ∞ in the good Stokes' wedges; all other curves turn around and are drawn into the bad Stokes' wedges. This remarkable behavior is illustrated in Fig. 3.

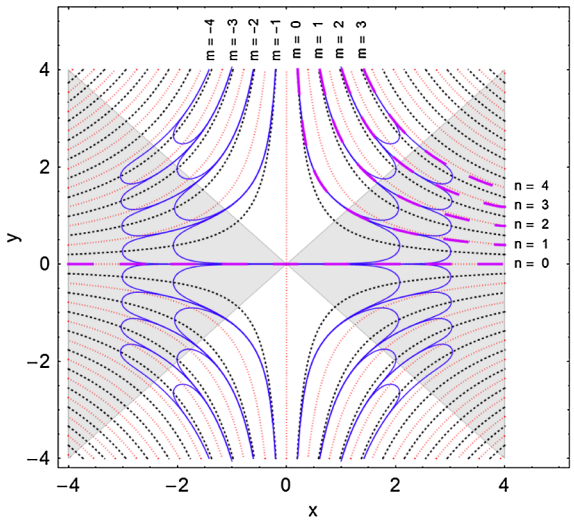

FIG. 3 (color online). Numerical solutions (solid curves) to the differential equation (6) in the complex-$z = x + iy$ plane. Solutions have vanishing slope on lightly dotted hyperbolas and infinite slope on heavily dotted hyperbolas. In the good Stokes' wedges (dark shading) $\rho(z)$ decays exponentially, and in the bad Stokes' wedges (unshaded) $\rho(z)$ grows exponentially. The only curves that reach $\pm\infty$ in the good wedges are separatrices (heavy dashed curves labeled $n = 0, \ldots, 4$). A typical solution curve in a good Stokes' wedge is unstable; as $x \to \infty$ the curve turns away from the separatrix, leaves the wedge, and is drawn into a bad Stokes' wedge. In the bad wedge curves are stable and continue on to $\pm i\infty$ in quantized bunches labeled by m. The only continuous unbroken curve connecting the two good wedges is the special separatrix on the real axis.

Figure 3 shows that the only continuous path connecting the two good Stokes' wedges follows the real axis. All other paths terminate in one good and one bad Stokes' wedge, and thus the probability integral (7) along such paths diverges. This instability of contours in the good Stokes' wedge in Fig. 3 is a serious and generic problem that must be overcome if we wish to extend the quantum probability density into the complex plane.

To overcome this apparently insurmountable problem, we show that if a contour satisfying (6) in the complex-z plane enters a bad Stokes' wedge along one path and then returns along a second path in the same quantized bundle, then the integral along the combined paths is actually convergent. This result is surprising because the integral along each path separately is exponentially divergent. To prove convergence, we examine the integral

$$I = \int_Y^\infty dy e^{y^2}\left(\frac{e^{-[u(y)]^2}}{\sin[2yu(y)]} - \frac{e^{-[v(y)]^2}}{\sin[2yv(y)]}\right), \qquad (10)$$

where $u(y)$ and $v(y)$ are two solutions to (6) in the same bunch (that is, having the same value of m). The leading asymptotic behaviors of these solutions are given in (9), and in fact the entire Poincaré asymptotic expansions of $u(y)$ and $v(y)$ are identical to all orders in powers of $1/y$. However, the difference $D(y) \equiv u(y) - v(y)$ is nonzero and is exponentially small

$$D(y) \sim Ke^{-y^2}[1 + (n + 1/2)^2\pi^2 y^{-2}/4 + \ldots] \qquad (11)$$

as $|y| \to \infty$, where K is an arbitrary constant. This result reflects the hyperasymptotic (asymptotics beyond all orders) content of (6) [19].

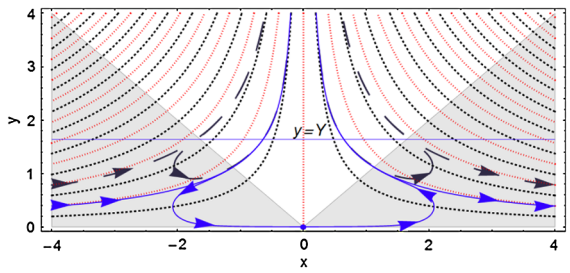

FIG. 4 (color online). Complex contours connecting good Stokes' wedges. A contour (solid curve) begins at $x = -\infty$ in the left good Stokes' wedge (shaded), leaves the wedge along a separatrix, and runs up to $i\infty$ in the bad Stokes' wedge (unshaded). The contour continues downward along a path in the same bunch, crosses the imaginary axis at $y = 0.003\,324\,973\,872\,707\,912$, and heads upwards into the same bad Stokes' wedge. Finally, the contour reemerges from the bad Stokes' wedge and continues towards $x = +\infty$ along a separatrix in the right good Stokes' wedge. Contours have zero slope on lightly dotted lines and infinite slope on heavily dotted lines. A second contour (dashed curve) connecting the two good Stokes' wedges visits the bad Stokes' wedge 4 times instead of twice.

Using (11), we approximate the integral (10):

$$I \sim K(-1)^n(n + 1/2)\int_Y^\infty dy y^{-3} \quad (Y \to \infty), \qquad (12)$$

which is convergent. Thus, while there is no continuous path running between the two good Stokes' wedges, there do exist paths connecting these wedges that repeatedly enter and reemerge from bad Stokes' wedges. On these contours the probability integral I in (7) exists. Several such paths are shown in Fig. 4.

Figure 5 is a generalization of Fig. 4 for the first excited state of the quantum harmonic oscillator. Note that contours that connect the two good Stokes' wedges may or may not pass through the node at the origin.

We do not present the argument in this Letter, but along the contours shown in Figs. 4 and 5 condition II in (4) is satisfied. That is, along the entire complex contour obeying the differential equation (6) the local contribution to the total probability integral is positive. Thus, the three conditions (3)–(5) are satisfied, and we have successfully extended the probabilistic interpretation of quantum mechanics into the complex plane.

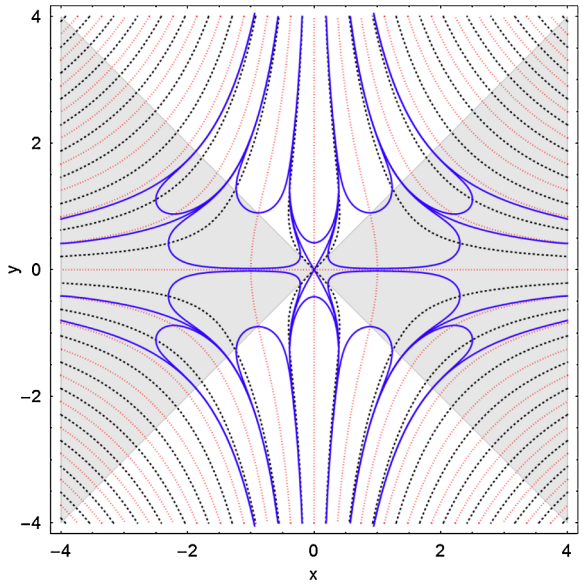

FIG. 5 (color online). Complex contours for the first excited state of the quantum harmonic oscillator. Four contours (solid lines) that begin at $x = -\infty$ in the left good Stokes' wedge (shaded) are shown. These contours leave this wedge along separatrices and run off to $\pm i\infty$ in the upper and lower bad Stokes' wedges (unshaded). After visiting a bad Stokes' wedge several times, the contours may pass through the node at the origin at 60° angles to the horizontal. At this node the probability density vanishes. Then the contours repeat the process in the right-half plane and eventually enter the right good Stokes' wedge along separatrices. It is also possible to have a complex contour that avoids the node at the origin and still connects the good Stokes' wedges. Solution curves are horizontal on lightly dotted lines and vertical on heavily dotted lines.

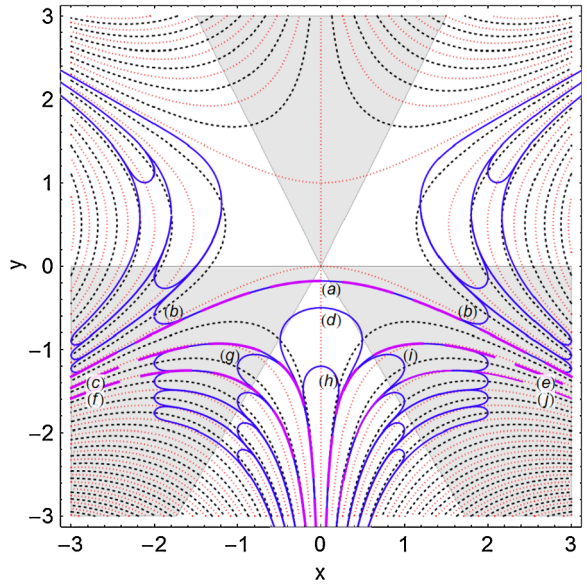

FIG. 6 (color online). Complex contours (heavy dashed lines) for the ground state ($J = 1$) of the quasi-exactly-solvable $\mathcal{PT}$ anharmonic oscillator. A separatrix (a) goes directly from the left good Stokes' wedge to the right good Stokes' wedge, crossing the imaginary axis at $y = -0.176\,651\,795\,619$. Paths (b) that cross $x = 0$ at higher points than the (a) path cannot reach ∞ in the good wedge. Because they are unstable, such paths turn around, enter the upper bad Stokes' wedges, and cannot reemerge. A separatrix (c) leaves the left good wedge. It enters the lower bad wedge to the left of $x = 0$, reemerges along paths (d) or (h), and reenters the bad wedge to the right of $x = 0$. It then continues into the right good wedge along the separatrix (e). Another separatrix (f) leaves the left good Stokes' wedge, enters the lower bad Stokes' wedge, leaves and returns along (g), leaves, reenters again along (d) or (h), leaves and reenters along (j), and finally enters the right good wedge along the separatrix (f). Solution paths are horizontal on lightly dotted lines and vertical on heavily dotted lines.

The analysis in this Letter is general and also extends to $\mathcal{PT}$ quantum theories, such as the quasiexactly solvable quartic anharmonic oscillator, whose Hamiltonian is $H = p^2 - x^4 + 2ix^3 + x^2 + 2iJx$ [20]. However, for quantum theories other than the harmonic oscillator, there are two kinds of bad Stokes' wedges: (i) wedges for which there exist probability contours C that enter and reemerge from the wedge and for which the probability integral along C converges, and (ii) wedges for which no such contour exists. For the Hamiltonian above there are three good Stokes' wedges and three bad Stokes' wedges, one of type (i) and two of type (ii) (see Fig. 6).

The quantum probability densities on the curves in Figs. 4–6 resemble pup tents with ripples in their canopies, in contrast to the smooth surface in the classical pup tent in Fig. 2. These figures are the complex analog of Fig. 1 and they provide a first glimpse of the complex correspondence principle. This work suggests several directions for further research. For example, a detailed study should be made of the high quantum-number limit, time-dependent contours C associated with noneigenstates (such as Gaussians) should be examined, and the complex correspondence principle for coherent states should be developed [21].

C. M. B. thanks the U.S. Department of Energy and D. W. H. thanks Symplectic Ltd. for financial support.

[1] C. M. Bender, S. Boettcher, and P. N. Meisinger, J. Math. Phys. (N.Y.) **40**, 2201 (1999).
[2] F. Calogero *et al.*, J. Phys. A **38**, 8873 (2005); Yu. Fedorov and D. Gomez-Ullate, Physica (Amsterdam) **227D**, 120 (2007).
[3] C. M. Bender, J.-H. Chen, D. W. Darg, and K. A. Milton, J. Phys. A **39**, 4219 (2006); C. M. Bender and D. W. Darg, J. Math. Phys. (N.Y.) **48**, 042703 (2007).
[4] C. M. Bender, D. D. Holm, and D. W. Hook, J. Phys. A **40**, F81 (2007); **40**, F793 (2007).
[5] A. Fring, J. Phys. A **40**, 4215 (2007).
[6] A. V. Smilga, J. Phys. A **42**, 095301 (2009).
[7] C. M. Bender *et al.*, Pramana J. Phys. **73**, 453 (2009).
[8] In the physical world the classically forbidden region is accessible. In optics, when the angle of incidence at an interface is less than a critical angle, there is no transmitted wave. The electromagnetic field crosses the boundary but is attenuated exponentially beyond the interface. This field does not vanish in the classically forbidden region, but there is no flux of energy; that is, the Poynting vector vanishes in the classically forbidden region. In complex classical mechanics particles enter the classically forbidden region but there is no particle flow parallel to the real axis; like the vanishing of energy flux in total internal reflection, the particle flux is orthogonal to the real axis. See J. D. Jackson, *Classical Electrodynamics* (John Wiley & Sons, Hoboken, 1999).
[9] C. M. Bender, D. C. Brody, and D. W. Hook, J. Phys. A **41**, 352003 (2008).
[10] C. M. Bender and S. Boettcher, Phys. Rev. Lett. **80**, 5243 (1998).
[11] P. Dorey, C. Dunning, and R. Tateo, J. Phys. A **34**, L391 (2001); **34**, 5679 (2001).
[12] A. Mostafazadeh, J. Math. Phys. (N.Y.) **43**, 205 (2002); **43**, 2814 (2002).
[13] C. M. Bender, D. C. Brody, and H. F. Jones, Phys. Rev. Lett. **89**, 270401 (2002); **92**, 119902 (2004).
[14] C. M. Bender, Contemp. Phys. **46**, 277 (2005); Rep. Prog. Phys. **70**, 947 (2007).
[15] P. Dorey, C. Dunning, and R. Tateo, J. Phys. A **40**, R205 (2007).
[16] Z. H. Musslimani *et al.*, Phys. Rev. Lett. **100**, 030402 (2008); K. G. Makris *et al.*, *ibid.* **100**, 103904 (2008).
[17] A. Guo *et al.*, Phys. Rev. Lett. **103**, 093902 (2009).
[18] C. E. Rüter *et al.*, Nature Phys., doi:10.1038/nphys1515 (2010).
[19] M. V. Berry and C. J. Howls, Proc. R. Soc. A **430**, 653 (1990).
[20] C. M. Bender and S. Boettcher, J. Phys. A **31**, L273 (1998).
[21] Coherent states for non-Hermitian $\mathcal{PT}$-symmetric potentials are discussed in E. M. Graefe, H. J. Korsch, and A. E. Niederle, Phys. Rev. Lett. **101**, 150408 (2008).